Numerical Investigation of the Transonic Base Flow of A Generic Rocket Configuration*

A. Henze, C. Glatzer, M. Meinke, W. Schröder
Institute of Aerodynamics, RWTH Aachen University, Germany

March 21, 2011

Numerical simulations of a high Reynolds number flow field of wind tunnel models of a generic rocket configuration were performed for transonic freestream conditions to improve the understanding of the highly intricate flow structures. The simulations demonstrate the applicability of the zonal RANS/LES approach for the rocket base flow. The configuration features a cylindrical sting support, thus representing a nozzle and allowing for investigations of a less disturbed wake flow. Since the Ma = 0.7 flow is the most critical regime as far as fluid structure interactions are concerned the paper concentrates on the transonic configuration. This wake flow is characterized by an expanding separated shear layer, the impact of which on the support leads to an increase in pressure, while the enclosed region, which determines the base drag, possesses a pressure minimum.

1. Introduction

A challenging problem in developing future reusable rocket-like launch vehicles is the understanding of the base flow. The flight regime of current and future launchers always includes subsonic, transonic, and supersonic speeds where the aerodynamic characteristics are strongly influenced by the flow in the base region. The freestream conditions, which represent selected stages of a real rocket launch, namely Ma = 0.2, 0.7 and 6.0, are of interest for an overall flow field analysis. However, the transonic flow at Mach = 0.7 represents the most critical regime in the launch trajectory, since the ambient pressure and density cause strong flow/structure interactions that could lead to mechanical failure of the nozzle. Therefore, it is of profound concern to understand the fundamental flow physics in the wake region. Although in simplified cases the base geometry is quite simple, the flow field remains highly complex. At supersonic speeds the base drag can exceed 35 % of the overall drag [11], and the subsonic base area of any generic wind tunnel rocket configuration is dominated by the interaction of the wake flow downstream of the main body with the freestream and the nozzle geometry. Since not all important flow features can be measured in experimental tests simultaneously, there is a basic demand for numerical simulations. In addition, the influence of a support for the wind tunnel model cannot be compensated, although the effect on the base flow can be significant.
Reynolds averaged Navier-Stokes (RANS) models are not capable of predicting accurate unsteady data and also fail to provide accurate results concerning the low pressure recirculation area behind the base, while the predictions of the attached flow around the main body are quite

*A. Henze at Institute of Aerodynamics, RWTH Aachen University, Wüllnerstraße 5a, 52062 Aachen., Germany

satisfactory. On the other hand, direct numerical simulations (DNS) are at the moment restricted to small Reynolds numbers and a small integration domain. Therefore, a zonal Reynolds averaged Navier-Stokes (RANS) / large eddy simulation (LES) approach is applied. RANS simulations are used to predict the attached main body flow field while LES computations are applied to the unsteady wake flow using the RANS results as inflow conditions. The turbulent viscosity of the RANS model is used to generate physical turbulent fluctuations at the inlet of the LES domain [6, 14].

2. Geometry and flow conditions

The transonic configuration of the rocket corresponds to a model that is used for experiments performed at Uni-BW Munich in the framework of the Collaborative Research Center/Transregio 40. The generic rocket consists of a rounded conical top with an apex angle of 36° and a cylindrical main body with a diameter of 108 mm. The nose radius spans 10 mm. The configuration possesses a cylindrical support mounted at the base of the main body, Fig. 1. This support sting mimics the contour of a nozzle and allows for investigations of an axially undisturbed base flow.

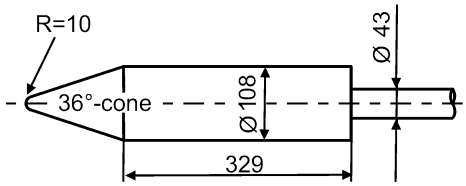

Fig. 1. Geometry of the generic rocket configuration with sting support

The flow conditions of the numerical simulations match the experimental data listed in Table 1.

Ma_∞	Re [1/m]	p_∞ [kPa]	p_0 [kPa]	T_∞ [K]	T_0 [K]	u_∞ [m/s]
0.7	$19 \cdot 10^6$	360	500	264	290	228

T a b l e 1. Transonic freestream flow conditions

3. Numerical approach

3.1. Zonal RANS/LES method

The compressible Naver-Stokes equations are solved in conservative form with a mixed central-upwind AUSM (advective upstream splitting method) scheme of second-order accuracy [8]. The fluxes and Mach numbers at the cell boundaries are determined by left and right interpolated variables obtained using the MUSCL approach according to van Leer [7]. The viscous terms are discretized by a central scheme of second-order accuracy. The temporal integration is performed

by an explicit 5-stage Runge-Kutta scheme of second-order accuracy, optimized for maximum stability of a central scheme. For the calculation of the base area an LES is performed, following the monotone integrated LES (MILES) approach [3]. No explicit subgrid scale (SGS) model is implemented, but the dissipation of the numerical scheme serves as an implicit SGS model [2]. For a detailed description of the flow solver the reader is referred to Meinke *et al.* [10].
The flow around the main body is simulated using the RANS model according to Spalart and Allmaras [12]. The results of the RANS solution close to the trailing edge of the main body are used as initial conditions for the base flow domain in which the LES method is used. The turbulent viscosity of the RANS model is used to generate physical turbulent fluctuations at the inlet of the LES domain [6, 14]. A body force is added to the wall-normal momentum equation on a number of control planes at different streamwise positions in order to match the turbulent flow properties of the LES with the given RANS values [5, 13]. To keep the transition zone between the RANS and LES domains small, the added synthetic turbulence accords to Jarrin *et al.* [4].

3.2. Computational Setup

For the transonic configuration, the integration domain is split into two sections. One domain covers the main rocket geometry, in which the RANS simulation is carried out and the second encompasses the sting support, thus capturing the highly time-dependent base area and the wake. The grid possesses a maximum resolution of $(\Delta x^+_{wall}, \Delta r^+_{wall}, \Delta\Phi^+_{wall}) = (500,\ 1,\ 150)$ within the RANS domain and of $(\Delta x^+_{wall}, \Delta r^+_{wall}, \Delta\Phi^+_{wall}) = (40,\ 1,\ 30)$ within the LES domain with x being the streamwise, r the wall-normal, and Φ the spanwise coordinate. Additional refinement is realized along the separating boundary layer and the free shear layer. The LES domain comprises a sector of 60° to save computational time. The grid extends to physical values of 2.5 D downstream of the base shoulder in the streamwise direction and 10 D in the radial direction. The grid points are equally distributed over 16 blocks to allow load-balancing for an efficient parallel computation. At solid walls an isothermal no-slip condition is imposed. Note that the simulations are compared to short time wind tunnel tests that lead to a negligible heating of the model. Periodic boundary conditions are used in the circumferential direction.

4. Transonic results

Since the transonic configuration of the rocket model includes an aft sting support, the main body flow remains undisturbed and thus is assumed axissymmetric. Fig. 2 and Fig. 3 show averaged and instantaneous Mach number distributions and pressure contours in the wake, respectively, in a streamwise cross section in the wake along the sting. Furthermore, the flow field is also described by streamlines. The averaging is performed over a dimensionless time of about 640 t corresponding to 160 ms, with t being the characteristic time defined as the time a particle of the freestream needs to cover the reference distance, i.e., the main body's diameter D. In Fig. 2 it is shown that the detached shear layer grows, while at the same time it slightly moves towards the centerline, such that it impacts the support between x/D = 1.5 and x/D = 2.5. It encloses a recirculation zone of low Mach number at the base. The center of the recirculating vortex with its low-pressure center can be located at about x/D = 0.7. The pressure drops to about half the freestream value, leading to an increase of the overall drag. The interaction of the shear layer with the support sting leads to an increase of static pressure downstream of the

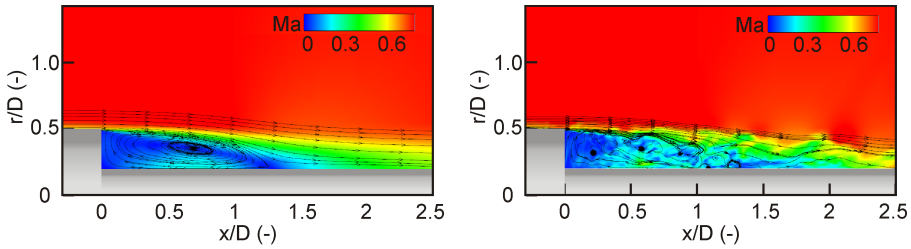

Fig. 2. Time-averaged and instantaneous Mach number distributions in the wake

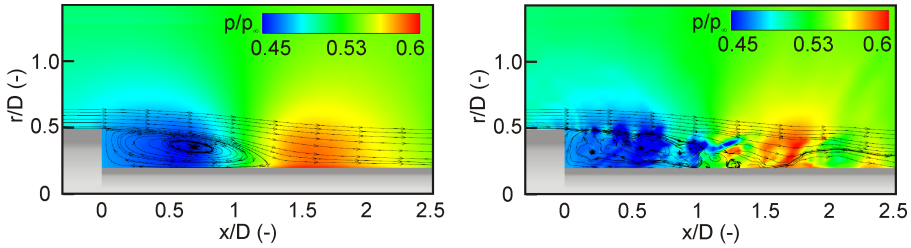

Fig. 3. Time-averaged and instantaneous pressure contours in the wake

rear stagnation point, which can be located at about x/D = 1.4. The pressure peaks at a value of about 0.6 of the static freestream pressure. The instantaneous flow plot in Fig. 3 indicates pressure fluctuations that are on the order of 10 % of p_∞. A comparison with the corresponding experimental data produced at Uni-BW Munich by Bitter *et al.* [1] showed good agreement.
Fig. 4 denotes distributions of the turbulent kinetic energy k at distinct positions in the wake. The highly turbulent shear layer impacts the sting and develops a wall-bounded layer. While eddies are convected further upstream within the base area the turbulent kinetic energy decays rapidly due to the viscous effects in the low Reynolds number base flow. In spite of the axi-

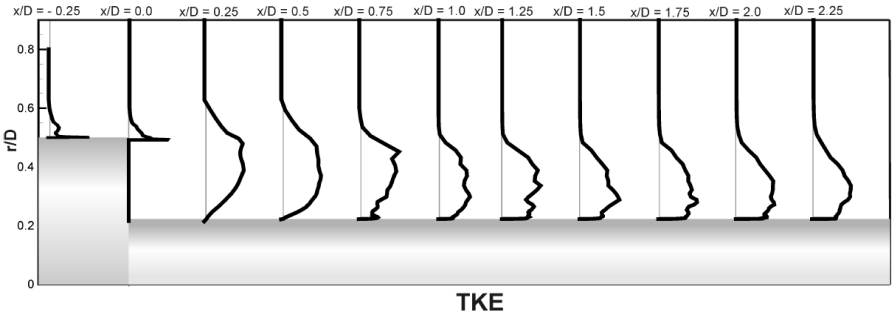

Fig. 4. Time-averaged turbulent kinetic energy at several streamwise locations

symmetric setup an azimuthal velocity component can be observed in Fig. 5. The temporally varying flow pattern are evidenced by streamlines and pressure contours due to turbulent fluctuations. The plane is taken at x/D = 0.5 behind the base shoulder. A time difference of 80 ms exists between each plot, thus evidencing a non-negligible mass flow in azimuthal direction and a behavior that is significantly different from an axisymmetric flow field.
The upper plot in Fig. 6 shows the Fourier transformed wall pressure signal for the posi-

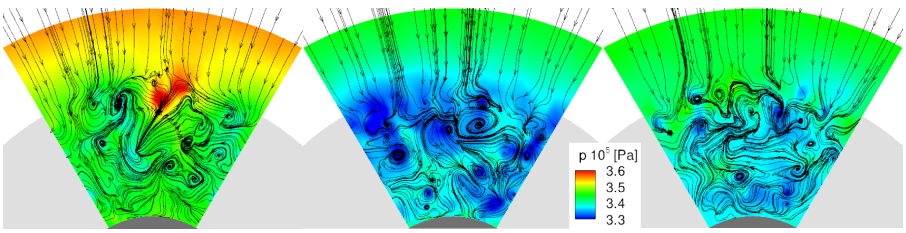

Fig. 5. Streamlines and pressure contours for several time levels (Δt = 80 ms, x/D = 0.5)

tion (x/D = 0, r/D = 0.46, Φ = 30°) near the separating boundary layer. The lower curve denotes the signal for (x/D = 0, r/D = 0.24, Φ = 30°) near the sting support. It is evident that the broadband noise, which is generated by the turbulent flow strucures, decreases at growing distance from the shear layer. In case of the high frequencies, which can be attributed to the turbulence generated in the free shear layer, the energy is dissipated in the vicinity of the base wall. Therefore, the lower pressure probe at the base wall hardly possesses any high frequency part. The low frequencies are caused by the large-scale vortical structures in the base, which characterize the global flow structure, but do not appear for a long-time interval. Only short-term periodic structures of varying frequency can be observed, which corresponds to experimental findings [1].

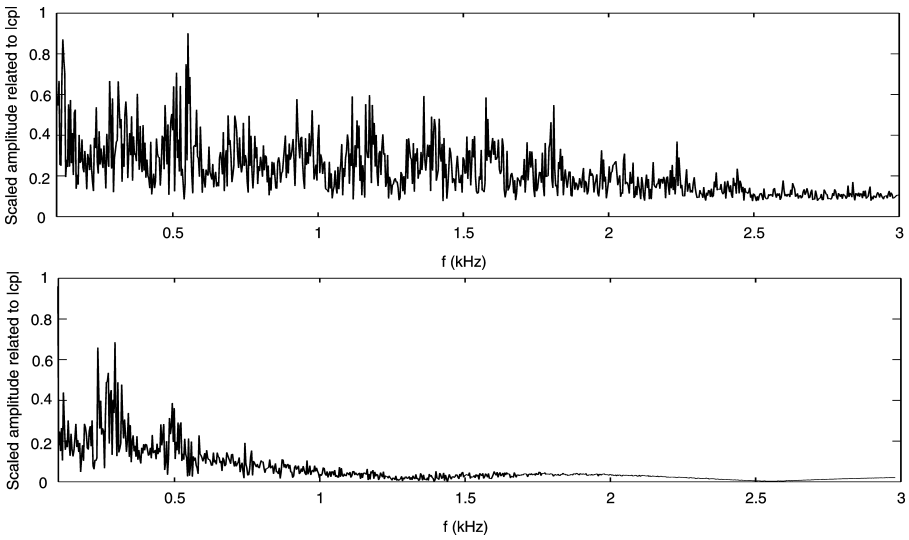

Fig. 6. Frequency analysis of temporal signals of the wall pressure at the base shoulder

5. Conclusion

The base flow behavior of a wind tunnel model of a generic rocket was investigated in the transonic flow regime using a zonal RANS/LES method. While the RANS approach was used to predict the attached flow field upstream the base, the LES was used to calculate the unsteady flow in the wake of the main body. The fundamental flow in the base and the near wake of the rocket was investigated using turbulent kinetic energy and frequency analyses. An instantaneous view on the base characteristics reveals a complex azimuthal flow structure even for

the axisymmetric geometry and a 60° simulation. Therefore an extensive 360° simulation of the wake flow is underway to give further insight into the highly complicated wake flow structures. Although few toroidal vortices and several larger and smaller scale eddies are identified at different times, they do not possess a preferred direction. As expected, a low pressure region forms in the range of the main recirculation vortex. The applied zonal RANS/LES method has been demonstrated to predict the intricate flow of high Reynolds numbers satisfactorily.

References

[1] Bitter M., Scharnowski S., Hain R., Kähler C.J., High repetition-rate PIV investigations on a generic rocket model in sub- and supersonic flows, Experiments in Fluids (2010)

[2] Boris J. P., Grinstein F. F., Oran E. S., Kolbe R. L., New insights into large eddy simulation, Fluid Dynamics Research, Vol. 10(4-6), pp. 199-228 (1992)

[3] Fureby C., Grinstein F. F., Large Eddy Simulations of High-Reynolds-Number Free and Wall-Bounded Flows, J. Comp. Physics, Vol. 181, pp. 6897 (2002)

[4] Jarrin N., Benhamadouche N., Laurence S., Prosser D., A synthetic-eddy-method for generating inflow conditions for large-eddy simulations, J. Heat and Fluid Flow, 27, pp. 585-593 (2006)

[5] Keating A., de Prisco G., Piomelli U., Interface conditions for hybrid RANS/LES calculation, International Journal of Heat and Fluid Flow, Vol. 27, pp. 777-788 (2006)

[6] König D., Meinke M., Schröder W., Embedded LES/RANS Boundary in Zonal Simulations, J. of Turbulence, Vol. 11, pp. 1-25 (2010)

[7] van Leer B., Towards the Ultimate Conservative Difference Scheme V. A Second-Order Sequel to Godunovs Method, J. Comp. Physics, Vol. 32, pp. 101136 (1979)

[8] Liou M. S., Steffen C. J., A New Flux Splitting Scheme, J. Comput. Phys., Vol. 107, pp. 23-39 (1993)

[9] Lueptow R., Turbulent boundary layer on a cylinder in axial flow, AIAA J., 28:17051706 (1990)

[10] Meinke M., Schröder W., Krause E., Rister T., A Comparison of Second- and Sixth-Order Methods for Large-Eddy Simulations, Computers and Fluids, Vol. 31, pp. 695-718 (2002)

[11] Rollstin L., Measurement of inflight base-pressure on an artillery-fired projectile, AIAA Paper, 287-2427 (1987)

[12] Spalart P. R., Allmaras S. R., A One-Equation Turbulence Model for Arodynamic Flows, AIAA Paper 92-0439 (1992)

[13] Spille A., Kaltenbach H.-J., Generation of turbulent inflow data with a prescribed shear-stress profile, Third AFSOR Conference on DNS and LES (2001)

[14] Zhang Q., W. Schröder, M. Meinke, A zonal RANS-LES method to determine the flow over a high-lift configuration, Computers and Fluids, Vol. 39, Issue 7, pp. 1241-1253 (2010)